MATHEMATICAL BIOSCIENCES AND ENGINEERING
Volume **14**, Number **1**, February **2017**

doi:10.3934/mbe.2017019
pp. **289–304**

ON A MATHEMATICAL MODEL OF BONE MARROW METASTATIC NICHE

Ana Isabel Muñoz

Departamento de Matemática Aplicada
Ciencia e Ingeniería de Materiales y Tecnología Electrónica
ESCET, Universidad Rey Juan Carlos, E28933, Móstoles, Madrid, Spain

J. Ignacio Tello*

1 Depto. Matemática Aplicada a las T.I.C. ETSI Sistemas Informáticos
Universidad Politécnica de Madrid. Madrid 28031, Spain
2 Centro de Simulación Computacional
Universidad Politécnica de Madrid. Boadilla del Monte, Madrid 28660, Spain

Abstract. We propose a mathematical model to describe tumor cells movement towards a metastasis location into the bone marrow considering the influence of chemotaxis inhibition due to the action of a drug. The model considers the evolution of the signaling molecules CXCL-12 secreted by osteoblasts (bone cells responsible of the mineralization of the bone) and PTHrP (secreted by tumor cells) which activates osteoblast growth. The model consists of a coupled system of second order PDEs describing the evolution of CXCL-12 and PTHrP, an ODE of logistic type to model the Osteoblasts density and an extra equation for each cancer cell. We also simulate the system to illustrate the qualitative behavior of the solutions. The numerical method of resolution is also presented in detail.

1. **Introduction.** *M*etastasis, (*meta*, "next", and *stasis* "placement") is the process by which a primary tumor spreads to a secondary distance location.

This process occurs in anatomical sites providing the necessary environment of vascularization, oxygen and food allowing to camouflage its action for triggering the fast growing of cancer.

The process presents several stages: Invasion to the surrounding extracellular matrix, intravasation, dissemination thorough the circulation system, extravasation in different organs, settlement into latency in a *pre-metastatic niche,* reactivation and generation of a new tumor. Only a small percentage of metastatic cancer cells survive to the circulation system, and those that get out of the circulatory system rapidly die if they can not find the appropriate micro environment.

Metastasis is the final stage of cancer and the major cause of death in patients with cancer. For that reason, many anticancer therapies focus on Metastasis inhibition. Thus anti-metastasis treatments have different targets depending on the stage of the process they act. Angiogenesis, Cancer Stem Cells and metastatic niche, the

2010 *Mathematics Subject Classification.* Primary: 35Q92; Secondary: 35R60.

Key words and phrases. Mathematical modeling of cancer, hematopoietic niche, osteoblast, CXCL-12, PTHrP, FEM.

The first author is supported by Project TEC2012-39095-C03-02, the second is supported by Project MTM2013-42907-P.

* Corresponding author: J. Ignacio Tello.

role played by the inmune system (promoting or inhibiting metastasis) are some of the interesting issues in the area at extracellular level.

The motivation of this work relies on creating a mathematical model to describe the tumor cells movement towards a metastasis location into the bone marrow and the influence of the inhibition of chemoattractant receptors in metastatic tumor cells due to the drugs action. The mathematical model shows the importance of the balance between the chemotactic and random movements to reach the pre-metastatic niche.

Prostate cancer skeletal involvement is a complicated process, in which bone provides a favorable medium for tumor growth, resulting in alterations in bone remodeling and development of cancer-associated bone lesions. Prostate cancer and the bone microenvironment communicate and interact with each other through the progression of skeletal metastasis.

The pre-metastatic niche is a microenvironment in a specific location which facilitates the invasion and survival of metastatic tumor cells and may host a secondary tumor once the metastatic cancer cells start to proliferate (see [12]). The pre-metastatic niche microenvironment is formed by different types of cells: endothelial cells, mesenchymal progenitor cells, cancer associated fibroblasts (CAFs), myeloid cells and osteoclast; chemical signals: CXCL-12 and TGF-β among others and the extracellular matrix (see [12] for more details).

Three different sources of metastatic niche have been already reported (see [12]):

1.- Native stem cell niches that metastatic cells may occupy in the host tissues;
2.- Niche functions provided by stromal cells not belonging to stem cell niches;
3.- Stem cell niche components that the cancer cells themselves may produce.

There exist at least two different types of pre-metastatic niches in the bone marrow, the osteoblast or endosteal niche and the vascular niche.

Osteoblast and osteoclast populations are the main agents involved in bone remodeling. In particular, osteoblasts mineralize the bone, while osteoclasts are responsible for bone resorption. There exists a dynamic equilibrium between osteoblasts and osteoclasts to maintain the bone tissue in normal adult vertebrates. This dynamical equilibrium existing in a healthy bone is perturbed by the chemical factors secreted by tumor cells.

The osteoblast niche is composed by osteoblast cells lining the endosteal surface which secretes a large variety of cytokines, growth factors and other signaling molecules that regulate the differentiation, the self-renewal and proliferation of hematopoietic stem cells (HSCs). The hematopoietic stem cells are a blood cell type which are host at the osteoblast niche in normal vertebrates (see [3]). The differentiation of HSCs produces myeloid cells, as macrophages, neutrophils, dendritic cells, etc, and lymphoid lineages as T-cells and B-cells among others.

Among the signaling molecules, CXCL-12, also known as stroma derivated factor 1 (SDF-1), is relatively highly expressed in the bone marrow (BM) (see [6]) and its receptor, CXCR-4, is expressed in HSCs and progenitors cells (see [9]). The retention in the BM of HSCs is regulated by the balance between CXCL-12 and Sphingosine-1-phosphate (S1P) produced by mature red blood cells in the circulatory system, which recruits HSCs to the circulation.

CXCL-12 is mainly produced by osteoblast cells, but it is also secreted by mesenchymal cells, endothelial precursor cells, cancer associated fibroblasts (CAFs) among others (see [13] and [16] for more details). The osteoblasts are activated

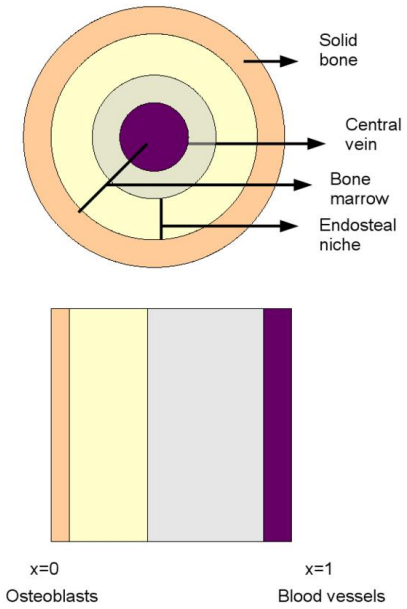

FIGURE 1. Geometry of the problem.

by parathyroid hormone (PTH) and PTH-related protein (PTHrP), through the PTH/PTHrP receptor (PPR) (see [2] and [3]).

Prostate cancer cells produce other pro-osteoblastic factors that enhance bone mineralization as wingless int (Wnt), transforming growth factor-β (TGF-β), vascular endothelial growth factor (VEGF), interleukin-6 (Il-6), prostate-specific antigen (PSA), bone morphogenetic protein (BMP), endothelin (ET), fibroblast growth factor 1 (FGF-1), FGF-2, FGF-8, insulin-like growth factor (IGF), osteoprotegerin (OPG), platelet-derived growth factor (PDGF), etc. Prostate cancer cells also produce pro-osteoclastic factors as RANK-L tumor necrosis factor α (TNFα), interluekin-1 (IL-1), IL-6, IL-8, IL-11, macrophage colony-stimulating factor (M-CSF), prostaglandin, etc.

It is known that CXCR-4 is overexpresed in metastatic solid tumor in prostate and breast cancer. The path CXCL-12 / CXCR-4 is used to localize the osteoblast niche (see [17]) and drives the cancer cells to the niche following the chemical gradients of CXCL-12 (chemotaxis).

Recently, several therapeutic strategies have been investigated to target the path CXCL-12/CXCR-4 to inhibit chemotactic movement (see for instance [7] and [11]). In [11], the authors present a novel therapeutic strategy and study the blockade of the path CXCL-12/CXCR-4 by AMD11070 in melanomas, comparing its effects with the inhibitor AMD3100. In this work, we consider the action of the inhibitor by reducing the chemosensitivity of the tumor cells, two different types of simulations are presented:

- when inhibitor is not present, and the tumor cell movement is composed of the combination of chemotaxis and random walk
- and when the action of chemotaxis is strongly reduced by the drug.

In the first case, the computational model shows how the tumor cell arrives at the niche while in the second case, the random movement is dominant and the cell doesn't arrive at the niche, at least during the computational time. The simulations show the existence of a threshold value in the rate chemotaxis / random coefficients: χ/D. Over such threshold value the cancer cell arrives at the niche and bellow it the cancer cell does not. The simulations show that the success of the therapy depends on the capacity to modify such rate by reducing the chemoattractant sensitivity.

In the following section, we introduce a mathematical model to describe the tumor cells movement towards a metastasis location into the BM. The description of the numerical scheme of resolution and some numerical simulations are performed in sections 3 and 4 respectively. The simulations illustrate the qualitative behavior of the solutions, which reproduce the migration of tumor cells from blood vessels to the osteoblastic niche in BM following the chemical gradients of CXCL-12.

2. **Mathematical model.**

In this section we present a mathematical model to describe tumor cells migration from blood vessels in BM to the osteoblast niche. The domain $\Omega := \{(x, y) \in [0, 1] \times [0, 1]\}$, represents a rescaled version of a cross section of the BM, between a blood vessel inside the bone ($x = 1$) and the compact bone surface ($x = 0$) where the osteoblast resides (see Figure 1).

We consider two different types of cells, osteoblasts, whose density shall be denoted by "b" and metastatic cancer cells (MCCs) and two diffusive unknowns, the CXCL-12 concentration, denoted by "w", and "u" which describes the tumor factors concentration, including osteoprotegerin (OPG), TGF-β and PTHrP among others.

2.1. **Metastatic cancer cells.**

We consider a finite number of MCCs, N, and denote its position by $(x_i, y_i) = (x_i(t), y_i(t))$ for $i = 1, ..., N$. We assume that the movement of the cancer cells is due to the combination of the action of the vector field generated by the gradient of the CXCL-12 concentration and a random walk term:

$$(x_i', y_i') = \chi(w)\nabla w(t, x_i(t), y_i(t)) + D(cos(2\pi\theta_{ij}(t)), sin(2\pi\theta_{ij}(t))) \qquad (1)$$

where $\chi(w)$ is the chemoattractant coefficient describing the cell sensitivity to CXCL-12, typically given by a decreasing function. For simplicity we take $\chi(w) = \chi_0/(1 + w)$ for a positive constant χ_0.The number $\theta_{ij}(t)$, for $t_j < t < t_{j+1}$, is a uniformly distributed random number in the interval $(0, 1)$ for a given increasing sequence of t_j. To initialize the model, the initial positions of the cancer cells $(x_i(0), y_i(0))$ are given.

Experiments show that cell movement is also influenced by the existing fibers in the extracellular matrix. On this occasion, to simplify the system we assume a homogeneous distribution of fibers in space and time and no influence in the cell movement.

Since the time from extravasation to the arrival of the pre-metastatic niche is small, we do not consider mitosis. Cancer cell death occurs if the cancer cell doesn$'$t reach the niche before a given time T.

2.2. **Tumor factors: PTHrP, TGF-β, osteoprotegerin, etc.** We denote by u the concentration of chemical factors secreted by prostate tumor cells, including osteoprotegerin (OPG), TGF-β and PTHrP. The secretion of the tumor factors comes from two sources: MCCs inside the BM at the positions (x_i, y_i) and the secretion from the primary tumor. The secretion from the tumor arrives at the BM through the existing blood vessels at the boundary of the domain, $x = 1$. The secretion from the MCCs is introduced by the term

$$\sum_{i=1}^{N} \frac{1}{2\sqrt{\pi\epsilon_i}} e^{-\frac{1}{4\epsilon_i}[(x-x_i(t))^2+(y-y_i(t))^2]}.$$

Notice that

$$\lim_{\epsilon_i \to 0} \frac{1}{\sqrt{2\pi\epsilon_i}} e^{-\frac{1}{4\epsilon_i}[(x-x_i(t))^2+(y-y_i(t))^2]} = \delta_{(x_i,y_i)}$$

where $\delta_{(x_i,y_i)}$ is the Dirac delta function. We shall consider a constant diffusion coefficient "D_u" and a constant degradation rate "μ_u", in the following equation:

$$u_t - D_u \Delta u + u\left(\mu_u + \frac{b}{1+u}\right) = \sum_{i=1}^{N} \frac{1}{\sqrt{2\pi\epsilon_i}} e^{-\frac{1}{4\epsilon_i}[(x-x_i(t))^2+(y-y_i(t))^2]}, \qquad (2)$$

which models the evolution of the concentration of tumor factors u. This equation is complemented with the initial datum:

$$u(0, x, y) = u_0(x, y), \quad (x, y) \in \bar{\Omega}$$

and the following boundary conditions

$$-D_u \frac{\partial u}{\partial n} = -F_u \qquad \text{at } x = 1, \qquad -D_u \frac{\partial u}{\partial n} = 0 \qquad \text{otherwise,}$$

where F_u is a positive constant. The term $bu/1 + u$, where b is the density of the osteoblast population, describes the consumption of u by osteoblasts. Notice that we assume that the osteoblast population is confined at the boundary $x = 0$.

2.3. **Osteoblast density.** Bone remodeling is regulated by osteoblasts located at the endosteal surface in dynamic equilibrium with osteoclasts, which are responsible of bone reabsorption. The process involves several substances and different types of progenitors cells in a basic multicellular unit (BMU). TGF-β activates osteoblast differentiation from mesenchymal precursors, increasing the bone formation (see [8]). Nuclear factor κB ligand (RANKL) and OPG are expressed by osteoblasts and regulate osteoclast activity. In [8], the authors propose a mathematical model considering two unknowns, the number of osteoclasts at the BMU and the number of osteoblasts, denoted by "c" and "b" respectively. The evolution of osteoblasts in [8] is given by the ODE:

$$b' = \alpha_2 c b^{g_{22}} - \beta_2 b, \qquad \alpha_2 = 4 \text{ day}^{-1}, \quad \beta_2 = 0.02 \text{ day}^{-1}, \qquad g_{22} \geq 0.$$

As before mentioned, we assume that osteoblast are located only at the boundary $x = 0$, and therefore b, the osteoblast density, is supposed to be a function of the spatial variable y. We consider that the osteoblast activation which depends on the TGF-β concentration is given by the equation:

$$b_t = g(b, u)b,$$

where g represents the growth rate of osteoblast, assumed logistic. To be precise, we shall consider the following equation for the evolution of b:

$$b_t = \alpha b \left(\mu_b + \mu_{bu} \frac{u}{1+u} - b \right). \tag{3}$$

where α is a proportionality constant and μ_b is the osteoblasts density at the equilibrium in the absence of TGF-β. The term $\mu_{bu} \frac{u}{1+u}$, results from considering that in the presence of TGF-β, the equilibrium is achieved at $b = \mu_b + f(u)$ for a non-negative and monotone increasing function f, satisfying $f(0) = 0$ and $\lim_{u\to\infty} f(u) = \mu_{bu}$ and assuming for simplicity that

$$f(u) = \mu_{bu} \frac{u}{1+u}.$$

Notice that we do not consider diffusion and transport of osteoblasts, see also [8]. The equation (3) is completed with an initial condition:

$$b(0, y) = b_0(y), \quad y \in [0, 1].$$

2.4. **CXCL-12 concentration.** CXCL-12 is secreted by osteoblasts, acting as a chemoattractant for the metastatic cancer cells which present CXCR-4 receptors at the surface. We denote by w the concentration of CXCL-12. Since the amount of cancer cells inside the BM is small, we neglect the loss of CXCL-12 due to the formation of the complex ligand-receptor CXCL-12 / CXCR-4 and its dissociation (see [5] for parameters values in CXCL-12 / CXCR-4 complex formation).

Hence, we assume that the evolution and distribution of w satisfies the parabolic equation

$$w_t - D_w \Delta w + \mu_w w = 0. \tag{4}$$

Diffusion of w has also been considered in [4], where degradation rates of CXCL-12 are considered to be of the order of $2 \times 10^{-5} s^{-1}$. We assume that CXCL-12 is only produced by osteoblast at the bone boundary (osteoblast niche), i.e. $x = 0$, and that the flux throughout the boundary is proportional to the osteoblast density, then the boundary conditions for (4) are:

$$-D_w \frac{\partial w}{\partial n} = -b, \qquad \text{at} \quad x = 0 \qquad \text{and} \quad -D_w \frac{\partial w}{\partial n} = 0, \qquad \text{otherwise.}$$

The problem is completed with a given initial datum,

$$w(0, x, y) = w_0(x, y), \quad (x, y) \in \bar{\Omega}.$$

3. **Numerical resolution.** In this section, we shall describe the numerical scheme of resolution of the system (1)-(4).

Due to the parabolic feature of the problem, we use a time marching scheme. Then, the solutions are computed with a decoupling iterative method. For this, we proceed to solve sequentially (1)-(4), in the following way: first, we solve the problem for the variable u (employing the positions obtained for the cells in the previous step), then, we pass to solve the problem for the variable b (by using the values obtained for u in the present step), next, we solve the problem for the variable w (considering the values of b in the present step) and, finally, we compute the location of the cells in the present step by using the just updated values of w.

The numerical resolution of the corresponding decoupled systems at each step in time will be carried out by means of well known methods. To be precise, the

resulting problems for the variables u and w are solved with a linear triangular finite-element method, and the problem for b with a semi-implicit Euler scheme.

Next, we shall briefly describe the overall process of resolution.

Let $t = T$ denote the final time of computation, let $P > 1$ be a natural number and let $\Delta t = T/P$ be the mesh step in the coordinate t. For $m = 0, 1, ..., P$, let $t_m = m\Delta t$ and define $u_m(x, y)$, $w_m(x, y)$, $b_m(y)$, $(x_{i,m}, y_{i,m})$ as follows:

$$u_m(x, y) = u(t_m, x, y),\ w_m(x, y) = w(t_m, x, y),\ b_m(y) = b(t_m, y)$$
$$\text{and} \quad (x_{i,m}, y_{i,m}) = (x_i(t_m), y_i(t_m)).$$

Notice that u_0, w_0, b_0 and $(x_{i,0}, y_{i,0})$ are given initial data. In order to discretizate with respect to the spatial coordinate, we will employ piecewise linear finite elements in an uniform triangular grid.

For each t_m, $m = 1, ..., P$, we consider the following uncoupled problems:

- Problem for u_m, the chemical factors secreted by prostate tumor cells:
  Given the location of the cells at the $m-$th level, b_{m-1} and u_{m-1}, determine u_m such that

$$\int_\Omega (1 + \Delta t\mu_u) u_m \phi dxdy + \Delta t D_u \int_\Omega \nabla u_m \nabla \phi dxdy$$
$$= \int_\Omega u_{m-1}\phi dxdy - \Delta t \int_\Omega \mu_u \frac{u_{m-1} b_{m-1}}{1 + u_{m-1}} dxdy$$
$$+\Delta t \sum_{i=1}^{N} \int_\Omega \frac{1}{2\sqrt{\pi\epsilon_i}} e^{-\frac{1}{4\epsilon_i}[(x-x_i(t))^2 + (y-y_i(t))^2]} \phi dxdy + \Delta t \int_{\Gamma_1} F_u \phi dy,\ \forall \phi \in H^1(\Omega),$$

  where N is the number of cells and Γ_1 is the boundary $x = 1$. Notice that $\phi \in H^1(\Omega)$ implies $\phi \in L^2(\Gamma_0)$ by the trace Theorem (see for example [1]).
- Problem for the osteoblast density:
  Given b_{m-1} and u_m, we consider a semi-implicit Euler scheme to determine the values of b_m at $x = 0$, that is to say

$$b_m = b_{m-1} + \Delta t \alpha b_{m-1} \left(\mu_b + \mu_{bu} \frac{u_m}{u_m + 1} - b_{m-1} \right).$$

- Problem for the concentration of CXCL-12 secreted by the osteoblasts:
  Given b_m and w_{m-1}, determine w_m such that

$$\int_\Omega (1 + \Delta t\mu_w) w_m \zeta dxdy + \Delta t D_w \int_\Omega \nabla u_m \nabla \zeta dxdy =$$
$$\int_\Omega w_{m-1}\zeta dxdy + \Delta t \int_{\Gamma_0} b_m \zeta dy,\ \forall \zeta \in H^1(\Omega),$$

  where Γ_0 is the boundary $x = 0$. Notice that $\zeta \in L^2(\Gamma_0)$.
- And finally, the location for the tumor cells is computed with the updated values of w at the m-th step in the following way:

$$(x_{i,m}, y_{i,m}) \approx (x_{i,m-1}, y_{i,m-1}) + \Delta t \chi(w_m) \nabla w_m(x_{i,m-1}, y_{i,m-1}) +$$
$$\Delta t D(cos(2\pi\theta_i(t_{m-1})), sin(2\pi\theta_i(t_{m-1}))),$$

  in the sense that the positions of the cells are restricted to grids points, and

$$P_{i,m-1} = (x_{i,m-1}, y_{i,m-1}) + \Delta t \chi(w_m) \nabla w_m(x_{i,m-1}, y_{i,m-1}) +$$
$$\Delta t D(cos(2\pi\theta_i(t_{m-1})), sin(2\pi\theta_i(t_{m-1})))$$

could not coincide with the coordinate of a grid point. To cope with this fact, we define $(x_{i,m}, y_{i,m})$ as the nearest grid point to the location given by $P_{i,m-1}$.

4. **Numerical simulations and biological interpretation.** In this section we present some numerical results and their biological interpretation in order to illustrate the dynamical behavior of the different variables.

As we mentioned in previous sections, we consider a square domain $\Omega = \{(x, y) \in [0, 1] \times [0, 1]\}$, which resembles a rescaled version of a cross section of the BM. The boundaries $x = 0$ and $x = 1$ represent the compact bone and the blood vessel boundary, respectively. The size of the step in time used in our simulations is $\Delta t = 10^{-4}$ and regarding the spatial discretization, we consider a structured triangular mesh with 101×101 spatial nodes.

We consider two scenarios in order to illustrate the effect of a therapeutic strategy consisting in targeting the path CXCL-12-CXCR-4 to inhibit chemotactic movement of the metastatic tumor cell. In the first scenario, we assume that no treatment has been applied and hence, the tumor cell movement is directed by a combination of chemotaxis and random walk. In this case the values of the parameters which we considered are:

$$\chi_0 = 10,\ D = 1,\ \mu_u = 1,\ \alpha = 1,\ \mu_b = 0.5,\ F_u = 10^{-5},\ \epsilon_i = 10^{-4},$$
$$\mu_{bu} = 100,\ \mu_w = 100 \text{ and } D_u = D_w = 5 \cdot 10^3. \tag{5}$$

In the second scenario, a drug is used to inhibit the chemoattractant action. In this case, the parameter values which were considered are:

$$\chi_0 = 0.01,\ D = 1,\ \mu_u = 1,\ \alpha = 1,\ \mu_b = 0.5,\ F_u = 10^{-5},\ \epsilon_i = 10^{-4},$$
$$\mu_{bu} = 100,\ \mu_w = 100 \text{ and } D_u = D_w = 5 \cdot 10^3. \tag{6}$$

In both scenarios, we assume that a cell, coming form the blood vessels, arrives in the domain and that is located initially at the point $(0.9, 0.6)$. We also consider that a niche is already established, and we consider that the initial profile for the osteoblast density is

$$b_0(y) = 10e^{-100(x-0.4)^2}.$$

The roles of the different parameters are the expected taking into account their positions in the equations.

- We observe the existence of a threshold value in the rate chemotaxis / random coefficients, χ/D, such that over the threshold value, the cancer cell arrives at the niche and bellow it the cancer cell does not. The simulations show that the success of the therapy depends on the capacity to modify the rate by reducing the chemoattractant sensitivity.
- Increasing the diffusion parameter D_w we obtain a faster response of the system. If the values of D_u are of order 1 and D_w is large enough, we also have a fast response, but in this case the values for the variables u and w increase considerably compared with the values obtained for D_u and D_w large.
- As expected, we have obtained that the value of μ_{bu} plays an important role in the qualitative behavior of b. Increasing μ_{bu} we obtain a higher production of b in case the cell arrived the niche and secretes tumor factors. Notice that it regulates the effect of the tumor factors on the osteoblast population.

- The role of the rest of the parameters are the expected.

In Figures 2-3, we illustrate the paths followed by the cells in both scenarios. We can observe that in the first case, the cells arrive at the niche, as there is no inhibition of the chemoattractant receptors, however in the second case ($\chi_0 = 0.01$) when a drug has been introduced to inhibit the action of the chemoattractant, the cell does not arrive at the niche and its movement is mainly directed by the random walk part. In Figures 2-3, at the bottom, we can observe in both cases, the evolution of the osteoblast density b, which shows increasing values over time in the first scenario, and decreasing values in the second one. Notice that the effect of the tumor factors u in b only takes place when the cell is already located at the niche.

In Figures 4-5, we present the results obtained for the tumor factors u in different times. In fact, we show the corresponding level curves to appreciate better the influence of the secretion term

$$\frac{1}{2\sqrt{\pi\epsilon_i}} e^{-\frac{1}{4\epsilon_i}[(x-x_i(t))^2+(y-y_i(t))^2]}$$

in the profile of u. We can observe that the region of bigger values of u is in correspondence with the position of the cell.

Finally, in Figures 6-7, we can see the results obtained for the CXCL-12 concentration, which resembles the behavior of b, depending on the scenario considered.

5. **Discussion.** We have presented a mathematical model to describe the tumor cells movement towards a metastasis location into the bone marrow and the influence of the inhibition of the chemoattractant receptors in the metastatic tumor cell due to the drugs action. Recently, several therapeutic strategies have been investigated to target the path CXCL-12 / CXCR-4 to inhibit chemotactic movement (see for instance [7] and [11]). In the model, we consider the evolution of signaling molecules CXCL-12 secreted by osteoblasts (bone cells responsible of the mineralization of the bone) and PTHrP (secreted by tumor cells) which activates osteoblast growth. The model consists of a coupled system of second order PDEs describing the evolution of CXCL-12 and PTHrP, an ODE of logistic type to model the osteoblasts density and an extra equation for each cancer cell. We simulate the system to illustrate the qualitative behavior of the solutions and the numerical method of resolution is presented in detail. In particular, we consider the following two scenarios to illustrate the effect of a therapeutic strategy which target the path CXCL-12/CXCR-4 to inhibit chemotactic movement of the tumor cell: The first scenario reflects the case where the inhibitor is not present, and the tumor cell movement is composed of the combination of chemotaxis and random walk. In the second scenario, the action of chemotaxis is strongly reduced by the drug used to inhibit the chemoattractant receptors. The simulations show the existence of a threshold value in the rate chemotaxis / random coefficients: χ/D. Over such threshold value the cancer cell arrives at the niche and below it the cancer cell does not. The simulations show that the success of the therapy depends on the capacity to modify such rate by reducing the chemoattractant sensitivity.

Acknowledgments. The first author would like to thank MEC of Spain for supporting Projects TEC2012-39095-C03-02 and MTM2014-57158-R, and the second author for supporting Project MTM2013-42907-P.

REFERENCES

[1] R. A. Adams, *Sobolev Spaces*, Academic Press, New York-London, 1975.

[2] A. A. Bryden, S. Islam, A. J. Freemont, J. H. Shanks, N. J. George and N. W. Clarke, Parathyroid hormone-related peptide: Expression in prostate cancer bone metastases, *Prostate Cancer Prostatic Dis*, **5** (2002), 59–62.

[3] L. M. Calvi, G. B. Adams, K. W. Weibrecht, J. M. Weber, D. P. Olson, M. C. Knight, R. P. Martin, E. Schipani, P. Divieti, F. R. Bringhurst, L. A. Milner, H. M. Kronenberg and D. T. Scadden, Osteoblastic cells regulate the haematopoietic stem cell niche, *Nature*, **425** (2003), 841–846.

[4] S. L. Chang, S. P. Cavnar, S. Takayama, G. D. Luker and J. J. Linderman, Cell, isoform, and environment factors shape gradients and modulate chemotaxis, *PLoS One*, **10** (2015), e0123450.

[5] N. L. Coggins, D. Trakimas, S. L. Chang, A. Ehrlich, P. Ray, K. E. Luker, J. J. Linderman and G. D. Luker, CXCR7 controls competition for recruitment of β-arrestin 2 in cells expressing both CXCR4 and CXCR7, *PLoS One*, **9** (2014), 841–846.

[6] K. Golan, O. Kollet and T. Lapidot, Dynamic cross talk between S1P and CXCL12 regulates hematopoietic stem cells migration, development and bone remodeling, *Pharmaceuticals*, **6** (2013), 1145–1169.

[7] G. Innamorati, M. T. Valenti, F. Giovinazzo, L. Dalle Carbonare, M. Parenti and C. Bassi, Molecular approaches to target gpcrs in cancer therapy, *Pharmaceuticals*, **4** 2011, 567–589.

[8] S. V. Komarova, R. J. Smith, S. J. Dixon, S. M. Sims and L. M. Wahlb, Mathematical model predicts a critical role for osteoclast autocrine regulation in the control of bone remodeling, *Bone*, **33** (2003), 206–215.

[9] A. J. Lilly, W. E. Johnson and C. M. Bunce, The haematopoietic stem cell niche: New insights into the mechanisms regulating haematopoietic stem cell behaviour, *Stem Cells International,* **2011** (2011), ID 274564.

[10] A. I. Muñoz, Numerical resolution of a model of tumor growth, *Mathematical Medicine and Biology*, **33** (2016), 1–29.

[11] G. O'Boyle, I. Swidenbank, H. Marshall, C. E. Barker, J. Armstrong, S. A. White, S. P. Fricker, R. Plummer, M. Wright and P. E. Lovat, Inhibition of CXCR4/CXCL12 chemotaxis in melanoma by AMD11070, *Br J Cancer.,* **108** (2013), 1634–1640, http://www.ncbi.nlm.nih.gov/pmc/articles/PMC3668477/

[12] T. Oskarsson, E. Batlle and J. Massague, Metastatic stem cells: Sources, niches, and vital pathways, *Cell Stem Cell*, **14** (2014), 306–321.

[13] A. A. Rose and P. M. Siegel, Emerging therapeutic targets in breast cancer bone metastasis, *Future Oncol.*, **6** (2010), 55–74.

[14] M. D. Ryser, N. Nigam and S. V. Komarova, Mathematical modeling of spatio-temporal dynamics of a single bone multicellular unit, *J. of Bone and Mineral Research*, **24** (2009), 860–870.

[15] J. Sceneay, M. J. Smyth and A. Möller, The pre-metastatic niche: Finding common ground, *Cancer Metastasis Rev.*, **32** (2013), 449–464.

[16] Y. X. Sun, J. Wang, C. E. Shelburne, D. E. Lopatin, A. M. Chinnaiyan, M. A. Rubin, K. J. Pienta and R. S. Taichman, Expression of CXCR4 and CXCL12 (SDF-1) in human prostate cancers (PCa) in vivo, *Journal of Cellular Biochemistry*, **89** (2003), 462–473.

[17] R. S. Taichman, C. Cooper, E. T. Keller, K. J. Pienta, N. S. Taichman and L. K. McCauley, Use of the stromal cell-derived factor-1/CXCR4 pathway in prostate cancer metastasis to bone, *Cancer Research*, **62** (2002), 1832–1837.

[18] J. I. Tello, On a mathematical model of tumor growth based on cancer stem cells, *Math. Biosc. Eng.,* **10** (2013), 263–278.

Received November 23, 2015; Accepted June 14, 2016.

E-mail address: anaisabel.munoz@urjc.es
E-mail address: j.tello@upm.es

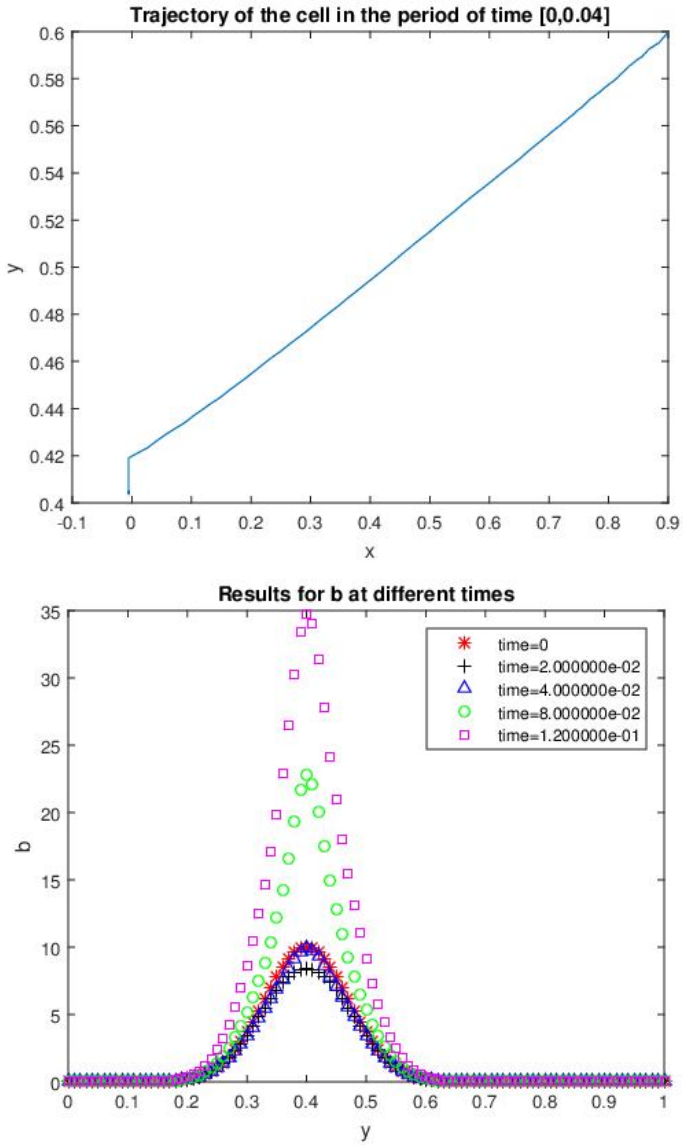

FIGURE 2. Results of the first scenario simulation, where therapeutic treatment had not been applied: Above we show the trajectory followed by the cell in the period of time [0,0.04]. At the bottom, there appear the results obtained for the osteoblast density at different times.

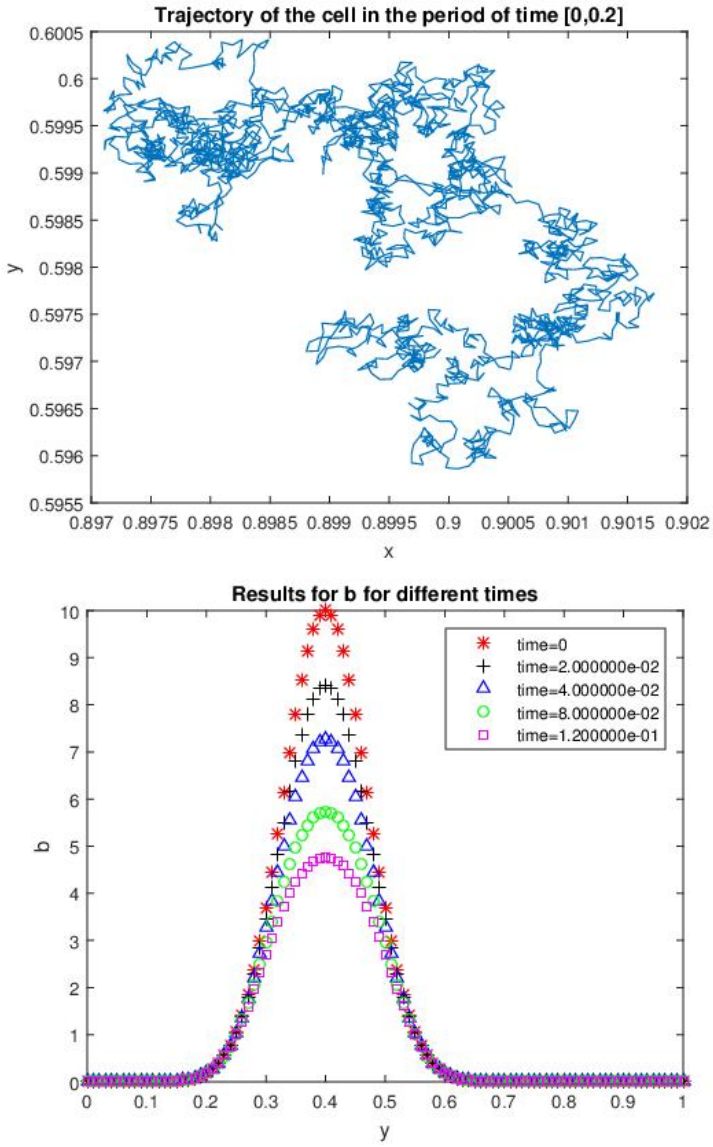

FIGURE 3. Results of the second scenario simulation, where a therapeutic treatment inhibiting the chemotactic movement of the cell is applied: Above it is depicted the trajectory of the cell in the period of time [0,0.2]. At the bottom, we illustrate the corresponding results for the osteoblast density at different times.

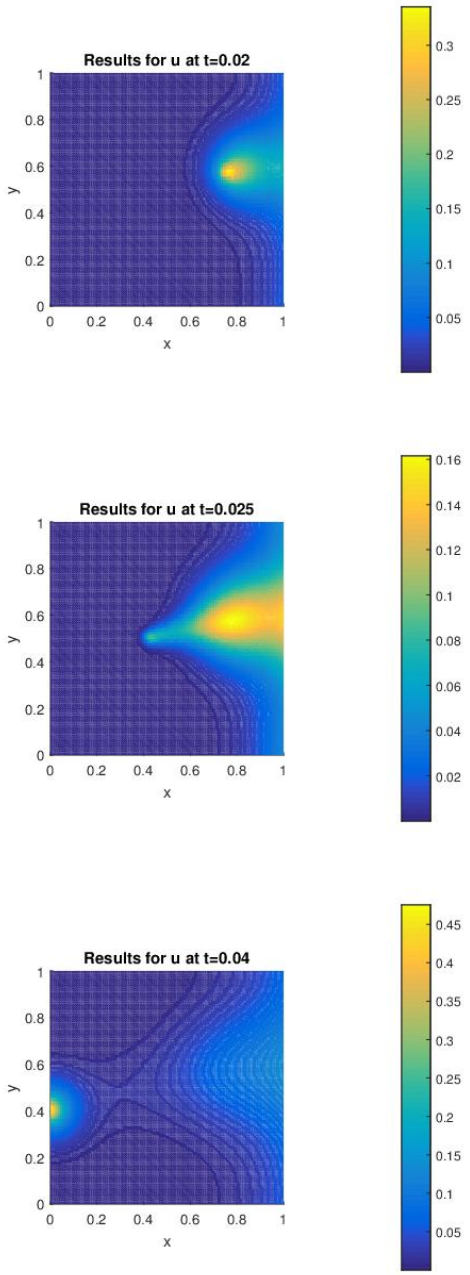

FIGURE 4. Results of the first scenario simulation regarding the evolution of the variable u, tumor factors. We show the corresponding the level curves of u for $t = 0.02$, 0.025 and 0.04.

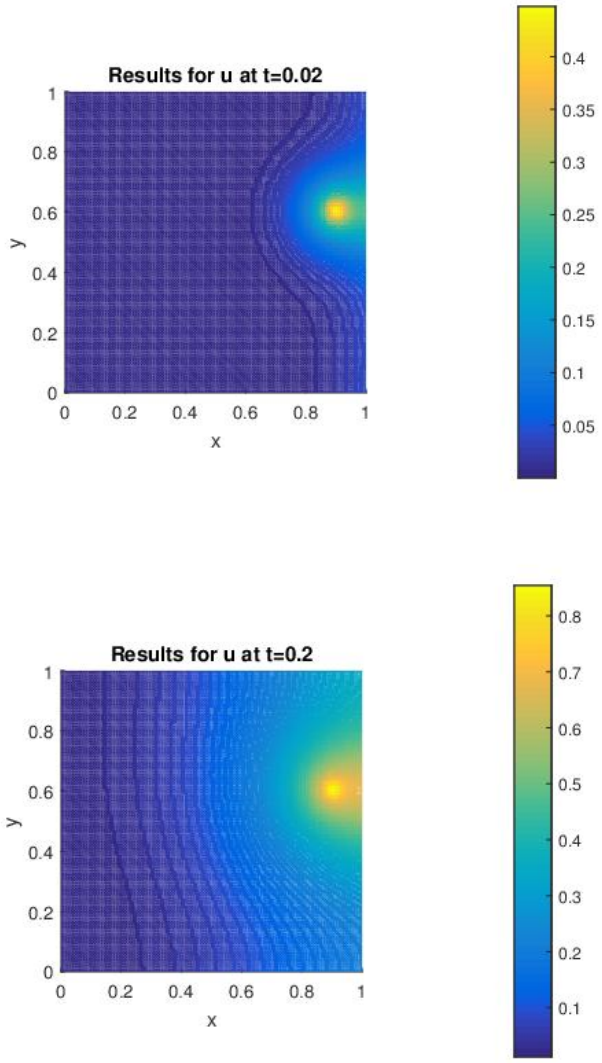

FIGURE 5. Results of the second scenario simulation for the variable u. We present the corresponding level curves at times $t = 0.02$ and $t = 0.2$.

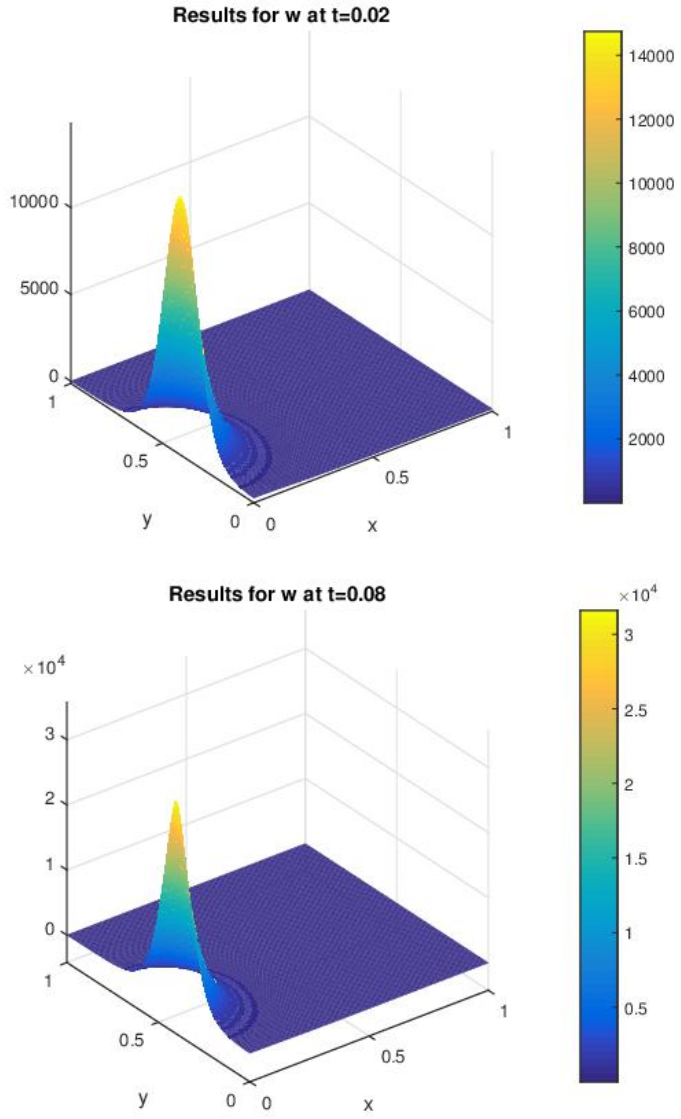

FIGURE 6. Results of the first scenario for the variable w, the chemoattractant CXCL-12 concentration at $t = 0.02$, when the cell has not reached the niche yet, and at time $t = 0.08$, when the cell is already well established in the niche.

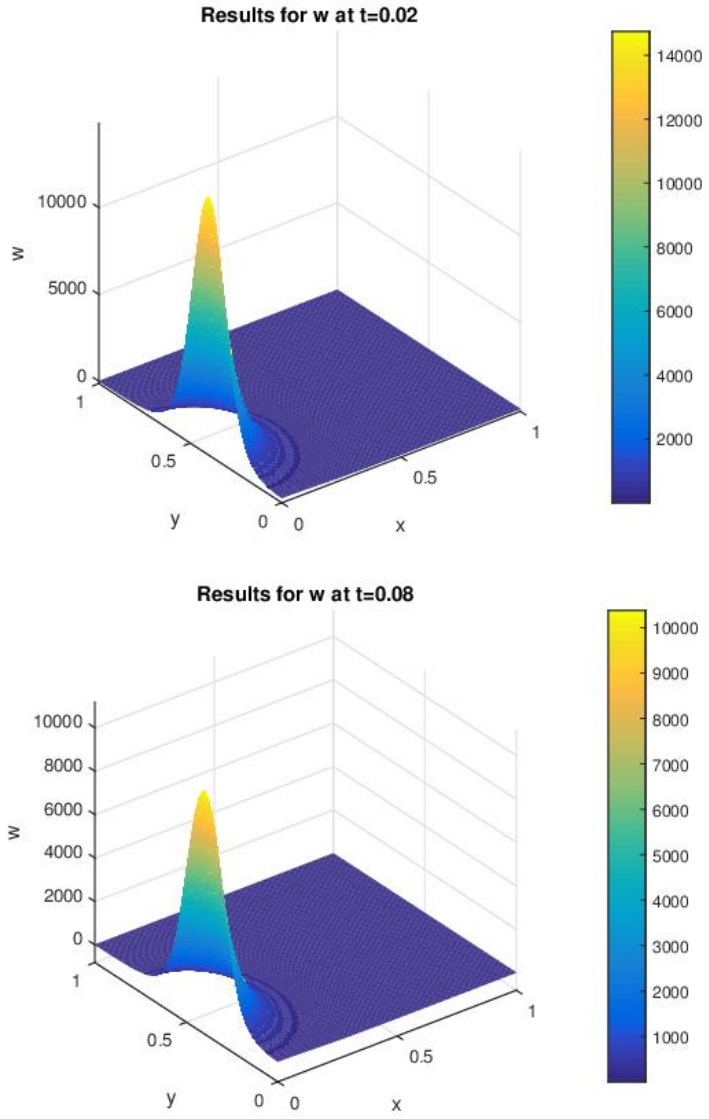

FIGURE 7. Results of the second scenario for the variable w, the chemoattractant CXCL-12 concentration at $t = 0.02$ and $t = 0.2$.